Determining the Minimal Required Ultra-Low-Dose CT Dose Level for Reliable Attenuation Correction of ^{18}F-FDG PET/CT: A Phantom Study

David W. Cheng[1], Monica Ghita[2], David Menard, CNMT[3], and Ming-Kai Chen[4]

[1]Jacobi Medical Center, Bronx, New York; [2]Department of Radiology, School of Medicine, Virginia Commonwealth University, Richmond, Virginia; [3]Division of Nuclear Medicine, Department of Diagnostic Radiology, Yale New Haven Hospital, New Haven, Connecticut; and [4]Department of Radiology and Biomedical Imaging, Yale University School of Medicine, New Haven, Connecticut

Our purpose was to investigate the minimal required submillisievert ultra-low-dose CT dose level and the corresponding tube current and voltage for reliable attenuation correction and semiquantitation in ^{18}F-FDG PET/CT in an effort toward radiation dose reduction. **Methods:** We performed a PET/CT investigational study using a National Electrical Manufacturers Association torso phantom containing 6 spheres (10, 13, 17, 22, 28, and 37 mm in diameter) filled with a fixed concentration of 60 kBq/mL and a background of 15 kBq/mL of ^{18}F-FDG. Two sets of PET images, separated by 2 h, were acquired for 3 min at a single bed position using 3-dimensional mode in a Discovery 690 scanner. Several sets of CT images were acquired for attenuation correction with different combinations of tube voltage (80, 100, and 120 kVp) and effective mAs (tube current–time product divided by pitch), using the maximum beam collimation (64 × 0.625 mm). The lowest CT dose acquisition technique available on this scanner is 10 mA, 0.4 s, and 1.375 for the tube current, tube rotation time, and pitch, respectively. The CT radiation dose was estimated on the basis of CT dose index volume measurements performed following the standard methodology and the Imaging Performance Assessment of CT Scanners (ImPACT) calculator. Each of the CT techniques was applied for attenuation correction to the same PET acquisition, using ordered-subset expectation maximization with 24 subsets and 2 iterations. The maximal and average radioactivity (kBq/mL) and SUVs of the spheres were measured. The minimal ultra-low-dose CT dose level for attenuation correction was determined by reproducible SUV measurements (±10%) compared with our reference CT protocol of 100 kVp and 80 mA for a 0.5-s rotation. **Results:** The minimal ultra-low-dose CT dose level for reproducible quantification in all spheres (<10% relative difference) was determined to be 0.3 mSv for a combination of 100 kVp and 10 mA at a 0.5-s rotation and a helical pitch of 0.984 (0.26 mGy measured CT dose index volume). From these results, we could confidently determine the CT parameters for reliable attenuation correction of PET images while significantly reducing the associated radiation dose. **Conclusion:** Our phantom study provided guidance in using ultra-low-dose CT for precise attenuation correction and semiquantification of ^{18}F-FDG PET imaging, which can further reduce the CT dose and radiation exposure to patients in clinical PET/CT studies. On the basis of the data, we can further reduce the radiation dose to the submillisievert level using an ultra-low-dose CT protocol for reliable attenuation correction in clinical ^{18}F-FDG PET/CT studies.

Key Words: research methods; adaptive statistical iterative reconstruction (ASIR); attenuation correction CT; phantom study; reliable SUV quantitation; submillisievert CT

Recent evidence from a retrospective large cohort study of over 178,600 United Kingdom residents with radiation exposure from CT scans in childhood assessed a relative risk of 3.18 for leukemia with a cumulative dose of more than 30 mGy, obtainable from as few as 5–10 head CT scans in patients under 15 y of age, and a relative risk of 2.82 for brain cancer with a cumulative dose of 50–74 mGy, obtainable from as few as 2–3 head CT scans, as compared with a low cumulative dose of less than 5 mGy (1). In a study of 680,000 Australians exposed to CT scans in childhood and adolescence, Mathews et al. reported an incidence rate ratio of 1.24 for all cancers with an observed dose–response relation of 0.16 per additional CT scan using an estimated average effective radiation dose of 4.5 mSv per scan (2). Therefore, the risk of cumulative radiation exposure from medical imaging could be substantial, especially for pediatric patients.

We recently published the results of a phantom study indicating the minimal radioactivity concentration for reproducible SUV_{max} (±10%) quantification to be 1.8 kBq/mL for an acquisition of 10 min, 3.7 kBq/mL for 3–5 min, 7.9 kBq/mL for 2 min, and 17.4 kBq/mL for 1 min with reference standards at a 10-min acquisition (3). In light of increased efforts to achieve submillisievert CT studies, iterative reconstruction techniques including adaptive statistical iterative reconstruction (GE Healthcare) and model-based iterative reconstruction (Veo; GE Healthcare) have been used to maintain image quality. Not without controversies (4,5), favorable reports have been published for coronary

CT angiography (*4–7*), chest CT (*8*) for pulmonary embolism (*9*), urinary tract stones (*10*), and CT colonography (*11,12*). Alternatively, dose reduction by sparse-sampled CT (*13*) was achieved in 10 patients by acquiring images at only 25% of the angular projections with subsequent reconstruction of the image data using an iterative algorithm. The authors reported no significant differences in detection of subcentimeter lung lesions between images reconstructed from standard-dose filtered backprojection, submillisievert filtered backprojection, and submillisievert iterative reconstruction, with equal confidence in reporting using the submillisievert iterative reconstruction technique. The scans were reported to be 0.25 mSv, or only one tenth the standard dose.

Although these computer algorithms may restore image quality for qualitative assessment, we are concerned about how ultra-low counts in submillisievert CT studies can affect the SUVs, if they are to be used for attenuation correction. The reproducibility of SUVs, a semiquantitative parameter widely used in clinical PET scans, is essential to assess the aggressiveness of disease and the response of disease to treatments in comparison studies. Since these algorithms are used during image reconstruction, the precision in SUVs is not expected to improve with the paucity of counts, unless quantitation software is modified. Souvatzoglou et al. (*14*) reported only a moderate correlation between the mean values in all segments using low-dose, ultra-low-dose, and slow CT for attenuation correction in 27 cardiac PET/CT scans, with no differences in scoring of qualitative assessment in the 3 groups. Xia et al. (*15*) investigated the feasibility of using ultra-low-dose CT for attenuation correction to reduce the additional radiation burden in respiratory motion compensation. We pursued basic measurements using a phantom over a wide range of CT attenuation scan settings in search of a minimal radiation dose threshold below which SUV determination may not be reliable.
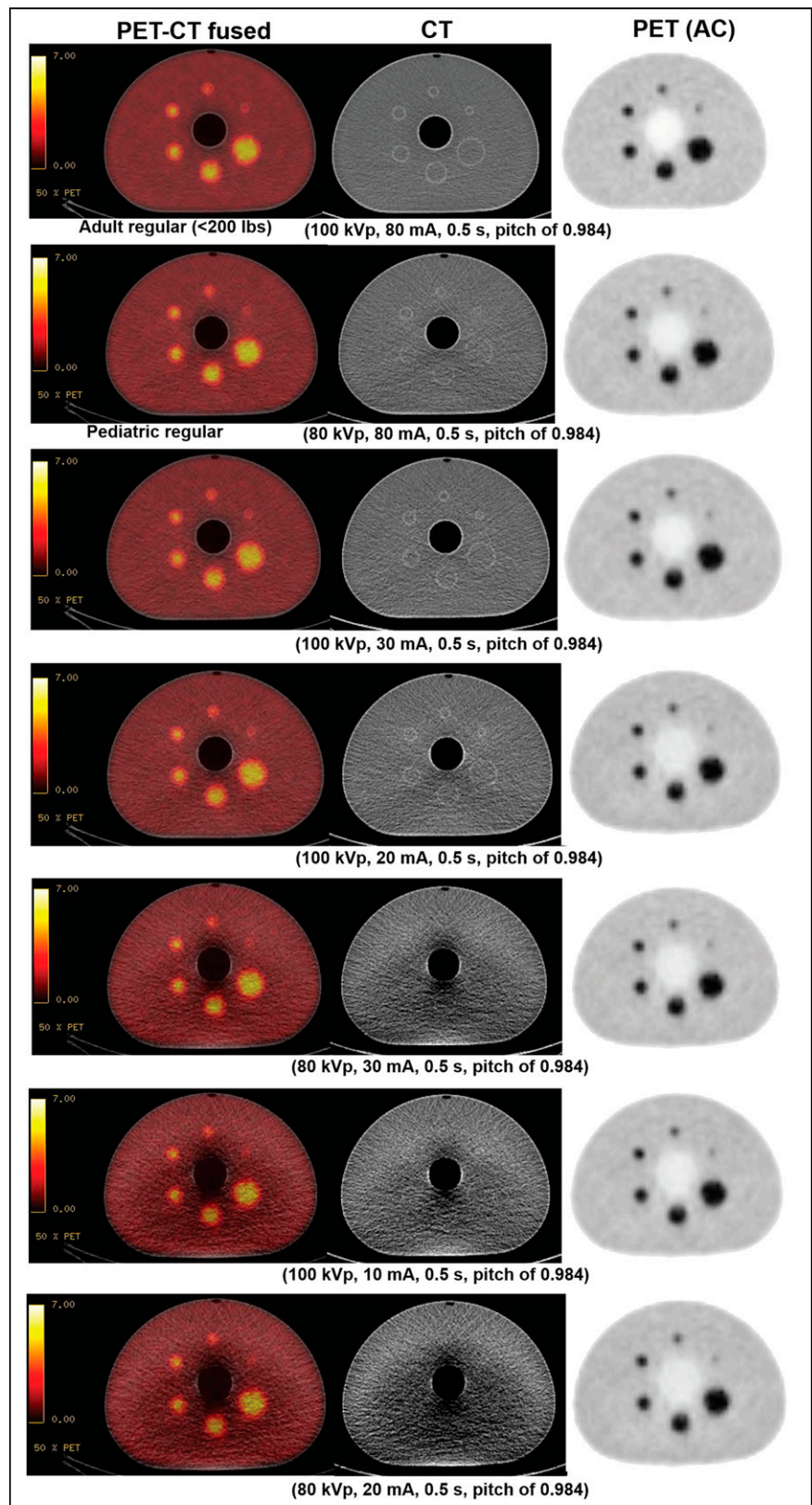

FIGURE 1. Representative images of PET (attenuation-corrected), CT, and PET/CT for phantom and spheres at various CT settings. CT settings of first and second rows are reference regular adult imaging protocol and pediatric imaging protocols, respectively, at Yale New Haven Hospital. In bottom 3 rows, delineation of spheres was not clear on CT images at lower radiation dose settings.

MATERIALS AND METHODS

A Discovery 690 (D-690) PET/CT scanner was used for the experiment (GE Healthcare). The D-690 is equipped with a lutetium-yttrium-orthosilicate detector and a 64-slice CT scanner, has a detection block of 54 (9 × 6) individual lutetium-yttrium-orthosilicate crystals (4.2 × 6.3 × 25 mm) coupled to a single squared photomultiplier tube with 4 anodes, and consists of 24 rings of detectors (total, 13,824 lutetium-yttrium-orthosilicate crystals) for an axial field of view of 157 mm. The transaxial field of view is 700 mm. The D-690 uses a low-energy threshold of 425 keV and a coincidence time window of 4.9 ns and operates in 3-dimensional mode only. The CT portion of the D-690 is a LightSpeed VCT with 912 channels × 64 rows, which allows full 360° rotation scans with variable time ranging from 0.35 to 2 s and reconstructed slice thicknesses of 0.625, 1.25, 2.5, 5, and 10 mm for the maximum fan-beam collimation of 40 mm.

We acquired PET/CT images using a National Electrical Manufacturers Association International Electrotechnical Commission phantom (Body Phantom Set; Data Spectrum Corp.) (Fig. 1), containing 6 hollow spheres (10, 13, 17, 22, 28, and 37 mm in diameter) filled with 60 kBq/mL in a background of 15 kBq/mL (a target-to-background ratio of 4:1) at the beginning and the end of a 2-h interval during the radioactive decay. PET images were acquired for 3 min at a single bed position in list mode using ordered-subset expectation maximization with 24 subsets and 2 iterations and a gaussian 2-mm filter using an Advantage Workstation (GE Healthcare) equipped with version 4.5 software. Multiple CT images were acquired for attenuation correction using different combinations of tube voltage (80, 100, and 120 kVp) and an effective tube current–time product mAs, at maximum beam collimation. The available settings to achieve the lowest effective dose were 10 mA, a 0.4-s rotation, and a pitch of 1.375. The CT images were reconstructed using conventional filtered backprojection. The adaptive statistical iterative reconstruction software for CT dose reduction was not available in our PET/CT scanner at the time of the study.

The radioactivity of the spheres with both SUV_{max} and average SUV (SUV_{ave}) was measured by applying sphere volumes of interest with a threshold of 41% of the maximal value in serial PET images using the Advantage Workstation. We coregistered CT images and adjusted the size of the volume of interest accordingly to make sure all volumes of interest were placed correctly. The SUV computation was derived from the radioactivity concentration (kBq/mL) divided by the total administered radioactivity within the phantom (kBq) and normalized to the total weight of the phantom. The variability of the SUV measurements in each sphere from the attenuation-corrected PET images using CT images with various combinations of tube current and voltage was calculated against the value in each sphere obtained using our standard clinical acquisition setting (100 kVp, 80 mA, 0.5-s rotation, and a helical pitch of 0.984) as the reference. A deviation in SUV (±10%) in comparison with the reference standard is considered acceptable in accordance with the test–retest variability of 20% for ^{18}F-FDG PET studies. Radiation dose estimation for CT scans was based on the CT dose index volume measured using the standard methodology (16) and the Imaging Performance Assessment of CT Scanners (ImPACT) CT patient dosimetry calculator, version 1.0.4 (17). The ImPACT CT dosimetry calculator is a computer software package that calculates organ and effective doses from CT examinations and makes use of the National Radiological Protection Board Monte Carlo
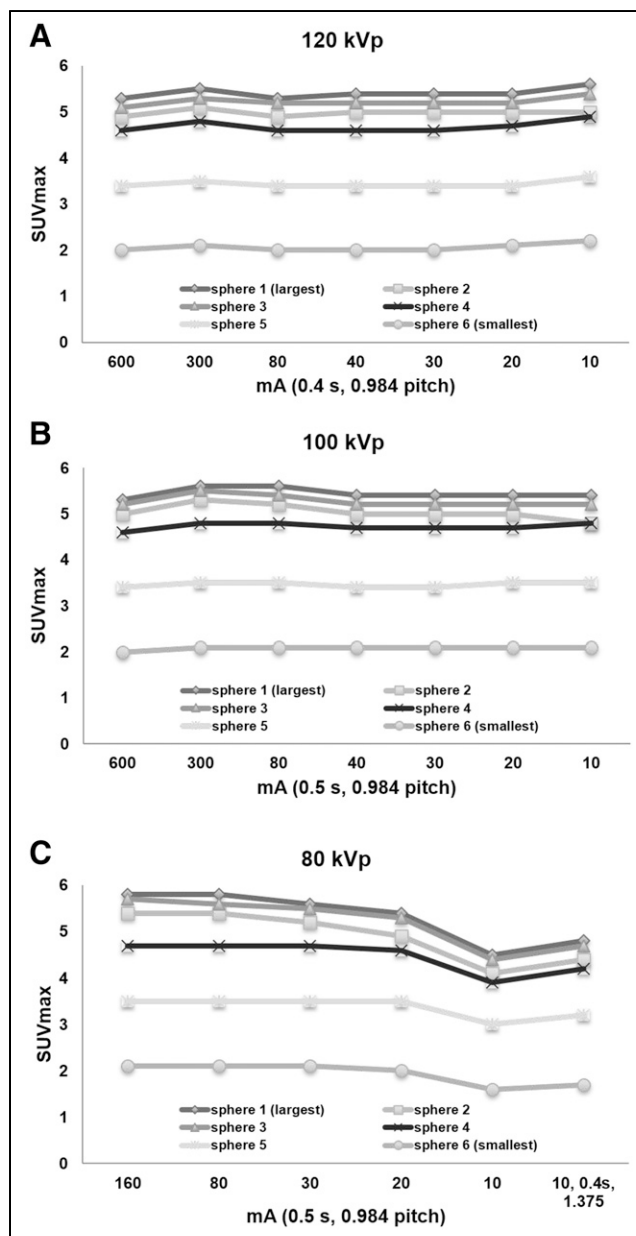

FIGURE 2. Impact on SUV_{max} from attenuation correction with various CT settings: 120 kVp (A), 100 kVp (B), and 80 kVp (C). Attenuation-corrected SUV_{max} measures are overall consistent for all spheres with CT settings of 120 kVp and 10–600 mA (A), 100 kVp and 10–600 mA (B), and 80 kVp and 30–160 mA (C). Attenuation-corrected SUV_{max} measures are slightly decreased (>10%) for some spheres with CT settings of 80 kVp and 10–20 mA (C).

published dose datasets (18). The Monte Carlo dose data provide normalized organ dose data for irradiation of a mathematic anthropomorphic phantom with a range of CT scanners, all of which are normalized to an isocenter air dose in the absence of any phantom. Since the particular output of the CT scanner in our PET/CT system is not included in the National Radiological Protection Board database, we selected from the database the model of our scanner (LightSpeed VCT) and manually input (the software provides this option) the measured CT dose index volumes for each individual CT attenuation scan to properly scale the normalized organ doses.
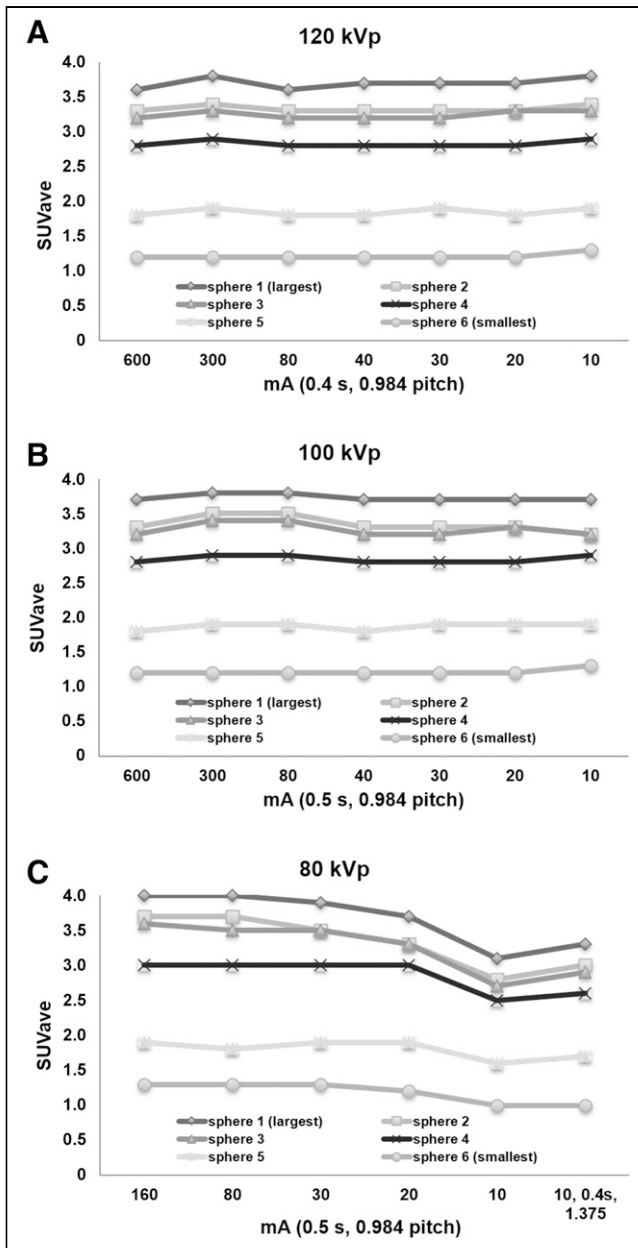
FIGURE 3. Impact on SUV$_{ave}$ from attenuation correction with various CT settings: 120 kVp (A), 100 kVp (B), and 80 kVp (C). Attenuation-corrected SUV$_{ave}$ measures are overall consistent for all spheres with CT settings of 120 kVp and 10–600 mA (A), 100 kVp and 10–600 mA (B), and 80 kVp and 30–160 mA (C). Attenuation-corrected SUV$_{ave}$ measures are slightly decreased (>10%) for some spheres with CT settings of 80 kVp and 10–20 mA (C).

TABLE 1
Estimated CT Doses (mGy) and Effective Doses (mSv) from Various Combinations of kVp and mA

kVp	mA	CT dose index volume (mGy)	mSv
120	600	19.61	32.4
120	300	10.18	16.2
120	80	2.63	4.3
120	40	1.32	2.2
120	30	0.99	1.6
120	20	0.66	1.1
120	10	0.33	0.5
100	600	15.25	20.6
100	300	7.68	10.3
100	80	2.06	2.7
100	40	1.03	1.4
100	30	0.77	1.0
100	20	0.55	0.7
100	10	0.26	0.3
80	160	1.73	2.7
80	80	0.87	1.4
80	30	0.43	0.5
80	20	0.22	0.3
80	10	0.11	0.2
80	10*	0.08	0.1

All 120-kVp CT scans use 0.4-s rotation time and pitch of 0.984. All 100- and 80-kVp CT scans use 0.5-s rotation time and pitch of 0.984, except for 0.4-s rotation time and pitch of 1.375, where noted by asterisk.

not significantly impacted by the low-dose CT setting (Fig. 1) or the low radioactivity of ^{18}F-FDG. However, we could not clearly delineate the spheres in CT images at the lower doses (Fig. 1, bottom 3 rows).

We also measured both SUV$_{max}$ and SUV$_{ave}$ within the spheres of the phantom from the attenuation-corrected PET images using the CT images with various combinations of kVp and mAs (Fig. 1). We found overall good consistency in SUV$_{max}$ and SUV$_{ave}$ measurements from attenuation-corrected PET images over a range of effective mAs (10–600 mA, 0.4- to 0.5-s rotation, and pitch of 0.984) at 120 kVp (Figs. 2A and 3A) and 100 kVp (Figs. 2B and 3B). We also found good consistency in SUV$_{max}$ and SUV$_{ave}$ ($\pm10\%$) measurements over the range of 30–160 mA with a 0.5-s rotation and a pitch of 0.984 at 80 kVp, below which we found a notable reduction (>10%) in SUV$_{max}$ and SUV$_{ave}$ at 10–20 mA, 0.5 s, and a pitch of 0.984 and at 10 mA, 0.4 s, and a pitch of 1.375 at 80 kVp (last 3 sets of measurement points in Figs. 2C and 3C). We repeated the PET and CT acquisition of the phantom after 2 h of radioactive decay and found good reproducibility.

We concluded that the minimum required radiation dose for the helical CT attenuation scan (pitch, 0.984) for precise quantification in all spheres ($\pm10\%$) was determined by the combination of 100 kVp, 10 mA, 0.5 s, and a pitch of 0.984, with a consequent 0.26-mGy measured CT dose index volume and 0.3-mSv estimated effective dose (Table 1).

RESULTS

We first performed visual assessments for all PET and CT images of the phantom and spheres (Fig. 1). We were able to identify the spheres clearly, including the smallest at 10 mm, in all the attenuation-corrected PET images with various CT settings, even for the lowest-dose technique after 2 h of radioactive decay. The detectability of PET was

DISCUSSION

Our phantom study explored lower limits within the sub-millisievert realm of ultra-low-dose CT used for attenuation correction required for reproducible semiquantification in ^{18}F-FDG PET imaging. We confirmed that the SUV measurements from the attenuation-corrected PET were consistent, even at very low dose settings of the CT. Therefore, we may confidently further reduce the current CT dose in routine clinical PET/CT studies without compromising the SUV measurements. One important clinical application is to reduce the CT dose in pediatric patients, as they are most susceptible to potential harm from unnecessary radiation exposure, although young adults and even all adults can benefit from a reduction in accumulated radiation dose.

The adequacy of CT-based attenuation correction for pediatric PET was evaluated previously using several phantoms (19). That study suggested that adequate attenuation correction can be obtained with very-low-dose CT (80 kVp, 5 mAs, pitch of 1.5:1) for pediatric patients and that such a correction can lead to a 100-fold dose reduction relative to diagnostic CT (19). Our current study also demonstrated the adequacy of CT-based attenuation correction with low-dose CT at a setting of 80 kVp, 15 mAs (30 mA with 0.5 s), and a pitch of 0.984, but we did notice more than a 10% reduction in SUV measurements at lower-dose CT settings and noticeable degradation of image quality impacting anatomic localization. The introduction of new iterative reconstruction algorithms in CT might allow a further reduction in the CT radiation dose settings while maintaining the image quality needed for anatomic localization. However, detailed quantitative image quality investigations using appropriate phantoms are needed to validate its feasibility. Weight-based, low-dose pediatric whole-body PET/CT protocols were proposed by the group at Seattle Children's Hospital (20). They used a weight-based adjusted ^{18}F-FDG dose for PET and weight-based categories for CT settings. The customized low-dose protocols could potentially reduce the radiation dose by 20%–50% from CT alone while maintaining diagnostic quality (20).

At the time this study was conducted, the standard CT settings for the D-690 at Yale New Haven Hospital were 80 mA, a 0.5-s rotation time, a pitch of 0.984, and 100 kVp for a standard adult with a body weight of 70 kg and 80 kVp for the pediatric protocol: 2.7 mSv and 1.4 mSv estimated effective doses, respectively. The CT images were reconstructed with conventional filtered backprojection, providing satisfactory imaging quality for anatomic localization.

On the basis of the results of this study, we could confidently reduce the radiation dose to the submillisievert level using an ultra-low-dose CT protocol for reliable attenuation correction and anatomic localization in clinical ^{18}F-FDG PET/CT studies.

In the current study, we focused only on the impact of PET SUV measures from ultra-low-dose CT. No image quality analysis was performed because this was beyond the purpose of the study. However, the impact of radiation dose reduction on image quality should be assessed if both reliable attenuation correction and accurate extraction of anatomic information are expected from the CT images of a PET/CT study. The new iterative reconstruction algorithms available for CT should be further investigated to improve the quality of ultra-low-dose CT images so as to provide acceptable anatomic information in PET/CT studies.

CONCLUSION

Our phantom study provided guidance in using ultra-low-dose CT for precise attenuation correction and semiquantification of ^{18}F-FDG PET imaging, which can further reduce the CT dose and radiation exposure to patients in clinical PET/CT studies. On the basis of the data, we can further reduce the radiation dose to the submillisievert level using an ultra-low-dose CT protocol for reliable attenuation correction in clinical ^{18}F-FDG PET/CT studies.

DISCLOSURE

No potential conflict of interest relevant to this article was reported.

KEY POINTS

QUESTION: What is the minimal required submillisievert-level dose for ultra-low-dose CT and the corresponding tube current and voltage for reliable attenuation correction and semiquantitation in ^{18}F-FDG PET/CT in an effort to reduce radiation dose?

PERTINENT FINDINGS: The minimal ultra-low-dose CT dose level for reproducible quantification in all spheres (<10% relative difference) was determined to be 0.3 mSv for a combination of 100 kVp and 10 mA at a 0.5-s rotation and a helical pitch of 0.984 (0.26 mGy measured CT dose index volume). Our phantom study provided guidance in using ultra-low-dose CT for precise attenuation correction and semiquantification of ^{18}F-FDG PET imaging.

IMPLICATIONS FOR PATIENT CARE: On the basis of the data, we can further reduce the radiation dose to the submillisievert level using an ultra-low-dose CT protocol for reliable attenuation correction in clinical ^{18}F-FDG PET/CT studies.

REFERENCES

1. Pearce MS, Salotti JA, Little MP, et al. Radiation exposure from CT scans in childhood and subsequent risk of leukaemia and brain tumours: a retrospective cohort study. *Lancet.* 2012;380:499–505.
2. Mathews JD, Forsythe AV, Brady Z, et al. Cancer risk in 680,000 people exposed to computed tomography scans in childhood or adolescence: data linkage study of 11 million Australians. *BMJ.* 2013;346:f2360.
3. Chen MK, Menard DH III, Cheng DW. Determining the minimal required radioactivity of ^{18}F-FDG for reliable semiquantification in PET/CT imaging: a phantom study. *J Nucl Med Technol.* 2016;44:26–30.
4. Heilbron BG, Leipsic J. Submillisievert coronary computed tomography angiography using adaptive statistical iterative reconstruction: a new reality. *Can J Cardiol.* 2010;26:35–36.
5. Behnes M, Haubenreisser H, Huseynov A, et al. Submillisievert ECG-gated whole thoracic CT-angiography for evaluation of a complex congenital heart defect in a young woman. *Int J Cardiol.* 2014;176:e54–e55.

6. Chen MY, Shanbhag SM, Arai AE. Submillisievert median radiation dose for coronary angiography with a second-generation 320-detector row CT scanner in 107 consecutive patients. *Radiology.* 2013;267:76–85.

7. Stehli J, Fuchs TA, Bull S, et al. Accuracy of coronary CT angiography using a submillisievert fraction of radiation exposure: comparison with invasive coronary angiography. *J Am Coll Cardiol.* 2014;64:772–780.

8. Khawaja RD, Singh S, Gilman M, et al. Computed tomography (CT) of the chest at less than 1 mSv: an ongoing prospective clinical trial of chest CT at submillisievert radiation doses with iterative model image reconstruction and iDose4 technique. *J Comput Assist Tomogr.* 2014;38:613–619.

9. Pontana F, Henry S, Duhamel A, et al. Impact of iterative reconstruction on the diagnosis of acute pulmonary embolism (PE) on reduced-dose chest CT angiograms. *Eur Radiol.* 2015;25:1182–1189.

10. Glazer DI, Maturen KE, Cohan RH, et al. Assessment of 1 mSv urinary tract stone CT with model-based iterative reconstruction. *AJR.* 2014;203:1230–1235.

11. Lambert L, Ourednicek P, Jahoda J, Lambertova A, Danes J. Model-based vs hybrid iterative reconstruction technique in ultralow-dose submillisievert CT colonography. *Br J Radiol.* 2015;88:20140667.

12. Gryspeerdt SS, Salazar P, Lefere P. Image quality improvement in submillisievert computed tomographic colonography using a fast 3-dimensional noise reduction method. *J Comput Assist Tomogr.* 2014;38:705–713.

13. Khawaja RD, Singh S, Lira D, et al. Role of compressive sensing technique in dose reduction for chest computed tomography: a prospective blinded clinical study. *J Comput Assist Tomogr.* 2014;38:760–767.

14. Souvatzoglou M, Bengel F, Busch R, et al. Attenuation correction in cardiac PET/CT with three different CT protocols: a comparison with conventional PET. *Eur J Nucl Med Mol Imaging.* 2007;34:1991–2000.

15. Xia T, Alessio AM, De Man B, Manjeshwar R, Asma E, Kinahan PE. Ultra-low dose CT attenuation correction for PET/CT. *Phys Med Biol.* 2012;57:309–328.

16. American Association of Physicists in Medicine Task Group Report 204: Size-Specific Dose Estimates (SSDE) in Pediatric and Adult Body CT Examinations. American Association of Physicists in Medicine; 2011.

17. ImPACT's ct dosimetry tool: CTDosimetry version 1.0.4. impactscan.org website. http://www.impactscan.org/ctdosimetry.htm. Accessed January 24, 2022.

18. Jones DG, Shrimpton PC. *Survey of CT Practice in the UK: Part 3.* National Radiological Protection Board; 1991.

19. Fahey FH, Palmer MR, Strauss KJ, Zimmerman RE, Badawi RD, Treves ST. Dosimetry and adequacy of CT-based attenuation correction for pediatric PET: phantom study. *Radiology.* 2007;243:96–104.

20. Alessio AM, Kinahan PE, Manchanda V, Ghioni V, Aldape L, Parisi MT. Weight-based, low-dose pediatric whole-body PET/CT protocols. *J Nucl Med.* 2009;50:1570–1577.